

# Anelastic deformation of Pb(Zr,Ti)O<sub>3</sub> thin films by non-180° ferroelectric domain wall movements during nanoindentation

M. Alguero,<sup>a)</sup> A. J. Bushby, and M. J. Reece

*Department of Materials, Queen Mary University of London, Mile End Road, London, E1 4NS United Kingdom*

A. Seifert

*Swiss Federal Institute of Technology, 1015 Lausanne, Switzerland*

(Received 7 January 2002; accepted for publication 8 May 2002)

Lead zirconate titanate Pb(Zr,Ti)O<sub>3</sub> ferroelectric thin films show significant anelastic deformation when indented with spherical tipped indenters. Experiments on films with different Zr/Ti ratio and a mixed  $\langle 001 \rangle, \langle 100 \rangle$  preferred crystallographic orientation have shown that there is a good agreement between the anelastic deformation and the maximum strain achievable by non-180° domain wall movement. An expected increase of the indentation stiffness of the films also accompanies the anelastic deformation because of the single crystal elastic anisotropy. All these observations seem to indicate that non-180° ferroelectric domain wall movements occur under indentation stresses and cause anelasticity. Stresses for maximum anelastic deformation are compared with those for recently reported stress-induced depolarization. © 2002 American Institute of Physics. [DOI: 10.1063/1.1491291]

The rapid growth of the field of microelectromechanical systems (MEMS)<sup>1</sup> has generated an intense research activity to develop techniques for the characterization of the mechanical properties of small volumes of materials<sup>2</sup> as depth sensing indentation.<sup>3,4</sup> Most of the initial work on nanoindentation was focused on silicon substrates.<sup>5</sup> Recent micro-Raman experiments on Si wafers have shown that phase transitions are induced by indentation.<sup>6</sup> These phenomena need to be understood if reliable mechanical parameters are to be extracted from the indentation penetration-force data.

MEMS sensors and actuators include an electromechanical transducer element. Piezoelectric thin films are usually chosen for high frequency applications,<sup>7</sup> among which ferroelectric lead zirconate titanate Pb(Zr,Ti)O<sub>3</sub> (PZT) has the highest piezoelectric coefficients.<sup>8</sup> Specific procedures for characterizing ferroelectric thin films using nanoindentation with spherical tipped indenters have recently been developed.<sup>9</sup> Their applicability rests on taking into account possible anelastic contributions to the penetration of the indenter in addition to the elastic and plastic ones. Anelasticity had been observed during uniaxial compression of PZT ceramics associated with the partially reversible movement of non-180° domain walls.<sup>10</sup> A significant anelastic contribution to the penetration has been observed during the indentation of lanthanum modified lead titanate Pb<sub>0.88</sub>La<sub>0.08</sub>TiO<sub>3</sub> (PTL) sol-gel films.<sup>9</sup> 90° domain wall movements were proposed to have caused the anelasticity.

We here report results on nanoindentation for three PZT films on Pt/TiO<sub>2</sub>/SiO<sub>2</sub>/Si substrates with Zr/Ti ratios of 0.30/0.70 (tetragonal with  $c/a = 1.018$ ), 0.45/0.55 (tetragonal with  $c/a = 1.008$ ), and 0.60/0.40 (rhombohedral), and with a thickness of 1 μm. The sol-gel processing was optimized to have the same microstructure, grain size ~80 nm, and mixed

$\langle 001 \rangle, \langle 100 \rangle$  preferred orientation.<sup>11</sup> The mixed  $\langle 001 \rangle, \langle 100 \rangle$  orientation fixed the angle between the normal to the 90°, 71°, and 109° domain walls and the indentation axis to ~45°, 90°, and 90°, respectively.

The experiments were accomplished with a UMIS 2000 nanoindentation system and a diamond spherical tipped indenter with a nominal radius of 7 μm. A typical experiment consisted of a series of 20 successive load-unload cycles at the same location, with each cycle in the series proceeding to a higher maximum force of up to 50 mN for the last cycle. The procedure used allowed the elastic, anelastic, and plastic components of the total penetration to be determined at the maximum force of each loop. This was done by analysing the unloading half cycle as follows. This half cycle was expressed as  $(F^{2/3}, h)$  and fitted to  $h = \alpha + \beta F^{2/3}$ . This is the expected behavior for an elastic-plastic contact where the unloading is assumed to be entirely elastic. For this case,  $\alpha$  corresponds to the depth of the residual impression after the indentation, and  $\beta F^{2/3}$  to the Hertzian elastic behavior.<sup>12</sup> This was the case for the PZT film with Zr/Ti = 0.60/0.40 and indentation forces below 30 mN, as it is shown in Fig. 1. However, the data for the other two films deviated from this behavior. An example for the film with Zr/Ti = 0.30/0.70 is also shown in Fig. 1. This implies an anelastic contribution to the deformation, which recovered during unloading. To analyze the data, it was assumed that this recovery did not start until the indentation force had decreased below a certain value. The purely elastic initial part of the unloading was isolated, and extrapolated to zero force, which provides the nonelastic (anelastic plus plastic) component,  $h_{ne}$ , of the penetration at maximum force. The plastic component,  $h_p$ , is just the residual depth and therefore,  $h_a = h_{ne} - h_p$  (as illustrated in Fig. 1). The slope of the elastic upper part of the unloading provides the effective indentation stiffness coefficient,  $E$ , of the film/substrate heterostructure at maximum load. The analysis was done for the 20 cycles of the series,

<sup>a)</sup>Present address: Instituto de Ciencia de Materiales de Madrid, CSIC, 28030 Madrid, Spain; electronic mail: malguero@icmm.csic.es.

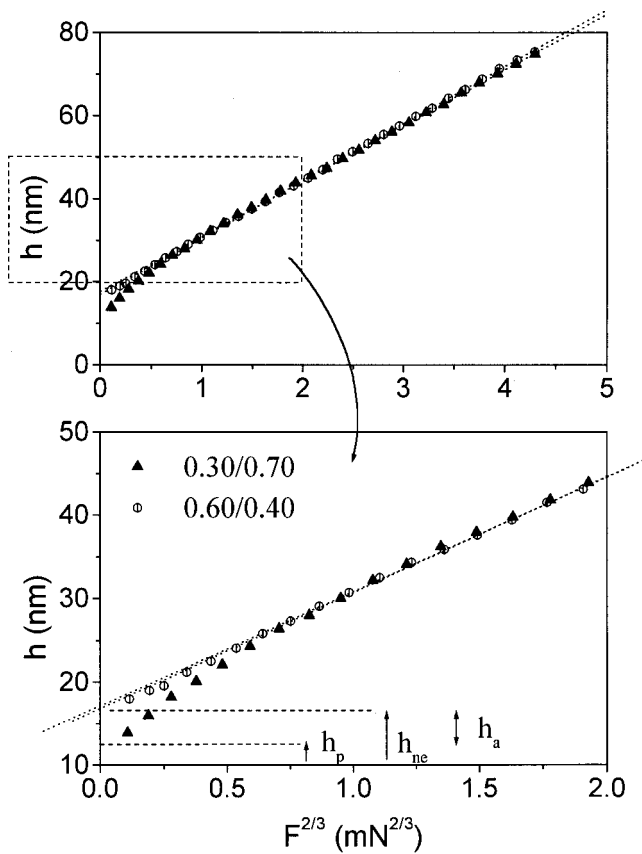


FIG. 1. Two examples, one showing anelasticity (for the film with Zr/Ti = 0.30/0.70) and one not showing it (for the film with Zr/Ti = 0.60/0.40), of the analysis of the unloading half cycle.

which provides  $h_a$ ,  $h_p$ , and  $E$  as a function of the indentation force. It is usual to express the penetration components as a function of the indentation stress,  $P_m$ , which is the mean pressure across the area of contact between the indenter and the sample, rather than as a function of  $F$ . It is also usual to express  $E$  as a function of the ratio between the radius of contact,  $a$ , and the film thickness,  $t$ . Nine locations were tested for each film. The maximum radius of the circle of contact in these experiments was  $1.63 \mu\text{m}$ .

The anelastic penetration data for four (out of the 9, for clarity) locations of the film with Zr/Ti = 0.30/0.70 are shown in Fig. 2(a) as a function of the indentation stress. The anelastic penetration,  $h_a$ , initially increased with the indentation stress for all the locations, up to  $\sim 7$  nm at  $\sim 4$  GPa. It then decreased for higher stresses to  $\sim 1$  nm at 5–6 GPa, to then increase again at even higher stresses. There is a significant dispersion of about 1–2 nm between the different locations, though the overall trends are very consistent. The average values for the three films are shown in Fig. 2(b). The trends are similar for the three films, though the maximum in  $h_a$  at  $\sim 4$  GPa decreases as Zr/Ti increases. It is 7, 5, and 2.5 nm for the 0.30/0.70, 0.45/0.55, and 0.60/0.40 films, respectively. For the initial increase in anelastic penetration, both the values and the behavior with the Zr/Ti ratio are consistent with what one would expect if the anelastic deformation was produced by the reversible movement of non- $180^\circ$  ferroelectric domain walls. The maximum contribution to the penetration that is achievable by  $90^\circ$  domain wall movements,  $h_{\text{dwm}}^{\text{max}}$ , for the films with the tetragonal structure and the

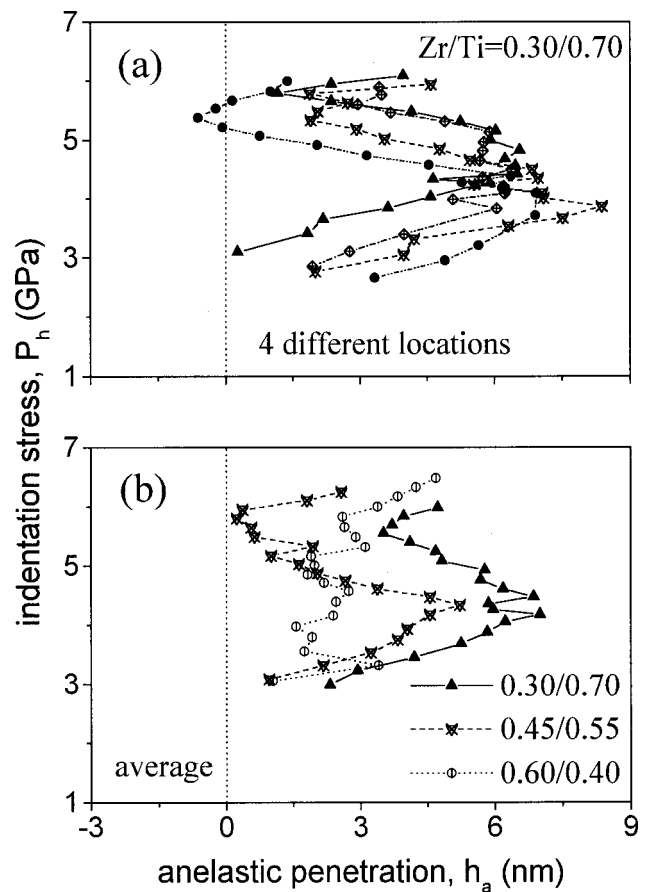


FIG. 2. (a) Anelastic component of the indenter penetration as a function of the indentation stress for four locations of the film with Zr/Ti = 0.30/0.70, and (b) average (over several locations) anelastic component for the three PZT films.

mixed  $\langle 001 \rangle, \langle 100 \rangle$  orientation is fully determined by the tetragonal distortion and the relative percentage of  $\langle 001 \rangle$  crystallites,  $x$ :

$$h_{\text{dwm}}^{\text{max}} = t \left( 1 - \frac{a}{c} \right) x. \quad (1)$$

Taking  $x = 1$  (full  $\langle 001 \rangle$  orientation) as a limit, Eq. (1) gives 18 nm for  $c/a = 1.018$ , and 8 nm for  $c/a = 1.008$ . However,  $x$  is not 1 for the PZT films and therefore, smaller values of  $h_a$  are obtained. Full  $\langle 001 \rangle$  orientation cannot be obtained on Si based substrates because of tensile stresses that develop at the film substrate interface during processing.<sup>13</sup> For the film with Zr/Ti = 0.60/0.40, which has rhombohedral structure,  $71^\circ$  and  $109^\circ$  domain walls are oriented unfavorably to the direction of the maximum shear stress. Also, the strain that they produce does not have a component in the  $z$  direction. For these reasons, hardly any anelasticity was observed. The decrease in  $h_a$  at greater stresses could be related to the wall movements becoming irreversible, i.e.,  $h_a$  becoming  $h_p$ . Unfortunately, other contributions to the plastic deformation masked this effect. The final increase in the anelastic penetration at the highest stresses occurred for the three compositions, and must be related to some other effect. Results on PTL films showed a similar behavior for the anelastic penetration when Pt/TiO<sub>2</sub>/Si substrates were used, but not when Ti/Pt/Ti/Si substrates were used.<sup>14</sup> TiO<sub>2</sub> layers are known to

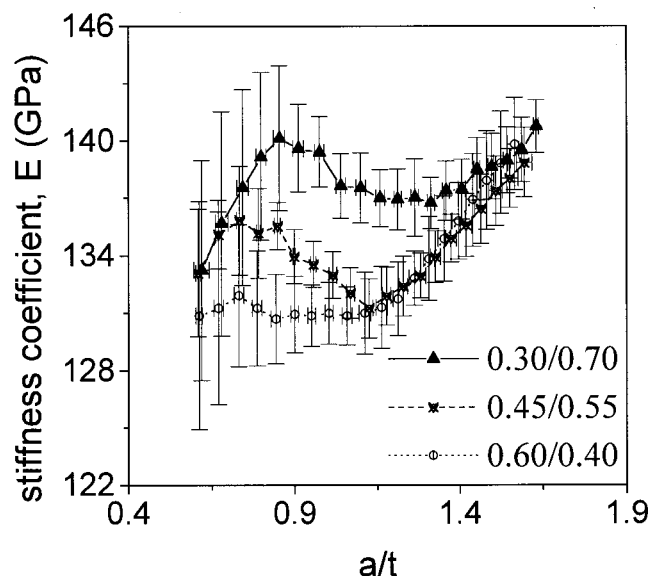


FIG. 3. Average indentation stiffness coefficient for the three PZT films as a function of the ratio between the radius of contact and the thickness.

be a worse adhesive than Ti layers for Pt/Si.<sup>15</sup> This suggests that the second increase in anelastic penetration could be related to an incipient delamination.

The effective indentation stiffness coefficient of the film/substrate heterostructure is shown in Fig. 3 as a function of  $a/t$ . This effective coefficient is that of the film when  $a/t \rightarrow 0$ , and that of the substrate when  $a/t \rightarrow \infty$  ( $a/t > 3$  is usually sufficient).<sup>16</sup> A stiffness coefficient of 93.5 GPa has been obtained in spherical indentation experiments on PZT-4 unpoled piezoceramics.<sup>17</sup> The expected coefficients for a range of PZT compositions around the morphotropic phase boundary between the tetragonal and rhombohedral structures ( $Zr/Ti=0.53/0.47$ ) were also generated in this work, from the literature values for the  $c_{ij}^E$  stiffness coefficients. Spherical indentation coefficients of 94 and 103 GPa were obtained for  $Zr/Ti=0.60/0.40$  and  $0.48/0.52$ , respectively. Values for smaller  $Zr/Ti$  were not given, though an extrapolation would give a value of 120 GPa for  $0.45/0.55$ . A value of 174 GPa is usually assumed for Si.<sup>16</sup> The expected behavior would then be a continuous increase from a value around 100–120 GPa for  $a/t=0$  to 174 GPa for  $a/t>3$ . However, the experimental curves obtained for the PZT films are not the expected ones, but are characterized by a maximum in the effective stiffness at  $a/t$  of between 0.7 and 0.9, which also corresponds to the indentation stress at the maximum anelastic deformation. This feature occurs when the stress field is mostly confined in the film ( $a/t < 1$ ), so it is probably not associated with the Pt/TiO<sub>2</sub>/SiO<sub>2</sub> heterostructure. The short circuit stiffness coefficient of PZT-4 piezoceramics has been shown to decrease from 93.5 to 76.2 GPa upon poling, which is associated with the reorientation of non-180° ferroelectric domains.<sup>17</sup> Therefore, the observed stiffening could be caused by domain reorientations through the reverse process. The initial rise in  $E$  for the three compositions increases with the elastic anisotropy of the composition (this anisotropy decreases as the  $Zr/Ti$  ratio increases).<sup>18</sup> This also supports the argument that it is caused by domain reorientation.

It has recently been reported that depolarisation occurs in ferroelectric thin films when indented with spheres.<sup>19</sup> Non-180° domain wall movements were proposed as the mechanism responsible of the phenomenon. It is thus interesting to compare the indentation stress at which the anelastic deformation reaches its maximum with the characteristic stresses for the depolarization of the films. The maximum anelastic deformation occurs at  $\sim 4$  GPa. The depolarization experiments were accomplished with a WC-Co cermet sphere with a 100  $\mu\text{m}$  radius and maximum forces of 500 mN. The corresponding indentation stress is 4.3 GPa, which is comparable with the one required to produce the maximum anelastic deformation.

Summing up, the presence of a maximum in the anelastic penetration indentation stress curve, the correlation between the anelastic penetration and the strain achievable by wall movements, the accompanying stiffening and its correlation with the single crystal elastic anisotropy indicate that the observed anelasticity is caused by reorientation of non-180° domains during indentation. This is further supported by the good agreement between the indentation stresses for anelasticity and for electrical depolarization.

<sup>1</sup>H. Fujita, Proc. MEMS'97, Nagoja, Japan, 1997, p. 1.

<sup>2</sup>S. M. Spearing, Acta Mater. **48**, 179 (2000).

<sup>3</sup>W. C. Oliver and G. M. Pharr, J. Mater. Res. **7**, 1564 (1992); N. X. Randall, C. Julia-Schmutz, J. M. Soro, J. von Stebut, and G. Zacharie, Thin Solid Films **308–309**, 297 (1997); Y. Y. Lim, M. M. Chaudhri, and Y. Enomoto, J. Mater. Res. **14**, 2314 (1999).

<sup>4</sup>M. V. Swain and J. Mencik, Thin Solid Films **253**, 204 (1994); J. S. Field and M. V. Swain, J. Mater. Res. **10**, 101 (1995); A. J. Bushby, Nondestr. Test. Eval. **17**, 213 (2001).

<sup>5</sup>G. M. Pharr, W. C. Oliver, and D. S. Harding, J. Mater. Res. **6**, 1129 (1991); T. Suzuki and T. Ohmura, Philos. Mag. A **74**, 1073 (1996); J. S. William, Y. Chen, J. Wong-Leung, A. Kerr, and M. V. Swain, J. Mater. Res. **14**, 2338 (1999).

<sup>6</sup>Y. G. Gogotsi, V. Domnich, S. N. Dub, A. Kailer, and K. G. Nickel, J. Mater. Res. **15**, 871 (2000); V. Domnich, Y. Gogotsi, and S. Dub, Appl. Phys. Lett. **76**, 2214 (2000).

<sup>7</sup>T. Fujii, S. Watanabe, M. Suzuki, and T. Fujii, J. Vac. Sci. Technol. B **13**, 1119 (1995); T. Maeder, P. Mural, L. Sagalowicz, I. Reaney, M. Kohli, A. Kholkin, and N. Setter, Appl. Phys. Lett. **68**, 776 (1996).

<sup>8</sup>H. D. Chen, K. R. Udayakumar, C. J. Gaskey, and L. E. Cross, Appl. Phys. Lett. **67**, 3411 (1995); A. L. Kholkin, E. L. Colla, A. K. Tagantsev, and D. V. Taylor, *ibid.* **68**, 2577 (1996).

<sup>9</sup>M. Algueró, A. J. Bushby, M. J. Reece, M. L. Calzada, and L. Pardo, Integr. Ferroelectr. **32**, 83 (2001); M. Algueró, A. J. Bushby, and M. J. Reece, J. Mater. Res. **16**, 993 (2001).

<sup>10</sup>H. Cao and A. G. Evans, J. Am. Ceram. Soc. **76**, 890 (1993).

<sup>11</sup>A. Seifert, N. Ledermann, S. Hiboux, J. Baborowski, P. Mural, and N. Setter, Integr. Ferroelectr. **35**, 159 (2001).

<sup>12</sup>B. R. Lawn, J. Am. Ceram. Soc. **81**, 1977 (1998).

<sup>13</sup>G. A. C. M. Spierings, G. J. M. Dormans, W. G. J. Moors, and M. J. E. Ulenaers, J. Appl. Phys. **78**, 1926 (1995).

<sup>14</sup>M. Algueró, A. J. Bushby, and M. J. Reece (unpublished).

<sup>15</sup>I. Kondo, T. Yoneyama, O. Takenaka, and A. Kinbara, J. Vac. Sci. Technol. A **10**, 3456 (1992).

<sup>16</sup>J. Menčík, D. Munz, E. Quandt, and E. R. Weppelmann, J. Mater. Res. **12**, 2475 (1997).

<sup>17</sup>U. Ramamurthy, S. Sridhar, A. E. Giannakopoulos, and S. Suresh, Acta Mater. **47**, 2417 (1999).

<sup>18</sup>B. Jaffe, W. R. Cook, and H. Jaffe, *Piezoelectric Ceramics* (Academic, New York, 1971).

<sup>19</sup>M. Algueró, A. J. Bushby, and M. J. Reece, Appl. Phys. Lett. **79**, 3830 (2001); M. Algueró, A. J. Bushby, P. Hvizdos, M. J. Reece, R. W. Whatmore, and Q. Zhang, Integr. Ferroelectr. **41**, 53 (2001).